Light-Driven Hydrogen Production by Hydrogenases and a Ru- Complex inside a Nanoporous Glass Plate under Aerobic External Conditions

ARTICLE *in* JOURNAL OF PHYSICAL CHEMISTRY LETTERS · JUNE 2014

Impact Factor: 7.46 · DOI: 10.1021/jz5008164

9 AUTHORS, INCLUDING:

Tomoyasu Noji
Nagoya Institute of Technology
18 PUBLICATIONS **60** CITATIONS
SEE PROFILE

Masaharu Kondo
Nagoya Institute of Technology
32 PUBLICATIONS **240** CITATIONS
SEE PROFILE

Yoshiki Higuchi
University of Hyogo
211 PUBLICATIONS **4,211** CITATIONS
SEE PROFILE

Shigeru Itoh
Nagoya University
222 PUBLICATIONS **4,121** CITATIONS
SEE PROFILE

THE JOURNAL OF PHYSICAL CHEMISTRY Letters

Letter

pubs.acs.org/JPCL

Light-Driven Hydrogen Production by Hydrogenases and a Ru-Complex inside a Nanoporous Glass Plate under Aerobic External Conditions

Tomoyasu Noji,*[,†] Masaharu Kondo,[‡] Tetsuro Jin,[§] Tetsuo Yazawa,[∥] Hisao Osuka,[⊥] Yoshiki Higuchi,[⊥,#] Mamoru Nango,[▽] Shigeru Itoh,[○] and Takehisa Dewa*[,†]

[†]Department of Frontier Materials, Graduate School of Engineering and [‡]Center for Fostering Young and Innovative Researchers, Nagoya Institute of Technology, Gokiso-cho, Showa-ku, Nagoya 466-8555, Japan

[§]Research Institute for Ubiquitous Energy Device, National Institute of Advanced Industrial Science and Technology (AIST), 1-8-31, Midorigaoka, Ikeda, Osaka 563-8577, Japan

[∥]Department of Materials Science and Chemistry, Graduate School of Engineering, University of Hyogo, 2167 Shosha, Himeji, Hyogo 671-2201, Japan

[⊥]Department of Life Science, Graduate School of Life Science, University of Hyogo, 3-2-1 Koto, Kamigori-cho, Ako-gun, Hyogo 678-1297, Japan

[#]CREST, Japan Science and Technology Agency, 4-1-8 Honcho, Kawaguchi-shi, Saitama 332-0012, Japan

[▽]The OCU Advanced Research Institute for Natural Science & Technology (OCARINA), Osaka City University, 3-3-138 Sugimoto, Sumiyoshi-ku, Osaka 558-8585, Japan

[○]Center for Gene Research, Nagoya University, Furo-cho, Chikusa-ku, Nagoya, Aichi 464-8602, Japan

Supporting Information

ABSTRACT: Hydrogenases are powerful catalysts for light-driven H_2 production using a combination of photosensitizers. However, except oxygen-tolerant hydrogenases, they are immediately deactivated under aerobic conditions. We report a light-driven H_2 evolution system that works stably even under aerobic conditions. A [NiFe]-hydrogenase from *Desulfovibrio vulgaris* Miyazaki F was immobilized inside nanoporous glass plates (PGPs) with a pore diameter of 50 nm together with a ruthenium complex and methyl viologen as a photosensitizer and an electron mediator, respectively. After immersion of PGP into the medium containing the catalytic components, an anaerobic environment automatically established inside the nanopores even under aerobic external conditions upon irradiation with solar-simulated light; this system constantly evolved H_2 with an efficiency of 3.7 μmol H_2 m^{-2} s^{-1}. The PGP system proposed in this work represents a promising first step toward the development of an O_2-tolerant solar energy conversion system.

SECTION: Surfaces, Interfaces, Porous Materials, and Catalysis

In recent years, the scientific community has shown an enormous interest in finding a method to efficiently produce sustainable and renewable hydrogen via light-driven water-splitting reactions, similar to those of natural photosynthesis.[1,2] Hydrogenase (H_2ase)-conjugated photosensitizers are major candidates for light-driven hydrogen production devices. While efficient under anaerobic conditions, O_2-sensitive H_2ases can be deactivated under aerobic conditions.[3] Solving this issue may advance the technology of devices and fuel cells for the light-driven hydrogen production, which may allow the use of water as an electron donor even with O_2 as a byproduct.[3−5] Several recent studies have proposed the use of various conjugates for the light-driven H_2 production, such as ruthenium (Ru) complex/TiO_2/H_2ase,[5] Ru complex-H_2ase conjugate,[6] photosystem I (PS I)/H_2ase,[7,8] and PS I/metal complexes,[9−12] some of which exhibited high turnover frequency. Berggren et al. reported that H_2ase, after being activated with synthetic di-iron components, can produce H_2 when reductants such as sodium dithionite/MV^{2+} are used.[13] However, these reactions were performed under either anaerobic or reducing conditions. In fact, only a few studies have shown examples of H_2ase that worked under aerobic conditions.[5,6,14−16] To achieve a sustainable and renewable production of hydrogen, the efficiency of H_2ase under aerobic conditions needs to be improved.[17,18]

Porous materials have enabled stable and dense immobilization of various enzymes[19] and photosynthetic pigment−protein complexes,[20−22] which can still function inside the porous

Received: April 25, 2014
Accepted: June 6, 2014
Published: June 6, 2014

environment. This approach renders substrates and products exchangeable.[20−22] In this work, we employed a porous glass plate (PGP) as a platform for light-driven hydrogen production. PGPs are transparent in the visible-near IR region (Figure S1 in the Supporting Information), possess size-controllable nanopores that penetrate the plate (Figure 1a), and show high

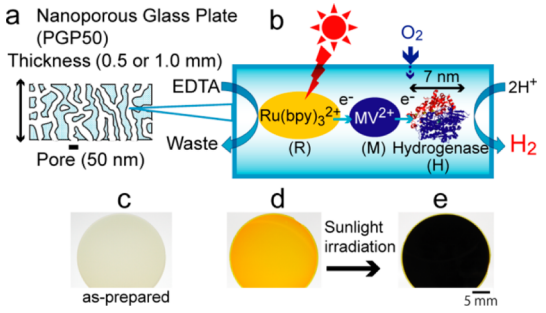

Figure 1. Light-driven H_2 production in nanopores. Schematic of nanoporous glass plate (PGP50) with pore diameter of 50 nm (a). $Ru(bpy)_3^{2+}$ (R, photosensitizer), MV^{2+} (M, electron mediator), and H_2ase (H) were immobilized in the PGP50, where efficient H_2 production took place via sequential electron transfer by redox components (b). Panels c−e: pictures of PGP50. (c) Photographic image of PGP50. (d) $Ru(bpy)_3^{2+}$(R)/MV^{2+}(M)-immobilized PGP50 (RM-PGP50). (e) Photoinduced reduction in RM-PGP50 in the presence of EDTA. Upon irradiation, RM-PGP50 changes color from yellow to black in a solution of 0.1 M Tris-HCl (pH 7.4) containing 20 mM EDTA under aerobic external conditions. Scale bar: 5 mm.

mechanical strength.[23−25] PGPs have been used as solid supports for enzymes and catalysts, photonic materials, and separation membranes.[25] In this study, through a simple and easy method, we have built a PGP-based device for light-driven H_2 production under ambient air conditions composed of [NiFe]-H_2ase (purified from *D. vulgaris* Miyazaki F, ∼89 kDa),[26] $Ru(bpy)_3^{2+}$ as a photosensitizer, and methyl viologen (MV^{2+}) as an electron mediator (Figure 1b).[27] In addition, we have demonstrated that this device provides an environment in which the ternary components (photosensitizer/mediator/H_2ase), immobilized to facilitate electron transfer reactions, are able to produce a significant amount of H_2 by addition of EDTA as a sacrificial electron donor even under aerobic external conditions.

In the present study, a PGP with an inner nanopore diameter of 50 nm (PGP50, Figure 1c), characterized by a sharp and monodisperse pore size distribution (Figure S2 in the Supporting Information), was employed. Yellowish RM-PGP50 ($Ru(bpy)_3^{2+}$/MV^{2+}-immobilized PGP50, Figure 1d) was formed after soaking PGP50 with $Ru(bpy)_3^{2+}$ (R) and MV^{2+} (M) for 24 h in a soaking solution (Figure S1 in the Supporting Information). $Ru(bpy)_3^{2+}$ was homogeneously absorbed in RM-PGP50 (Figure S3 in the Supporting Information). H_2ase-immobilized PGP50 (H-PGP50) was prepared by immersing PGP50 in an aqueous solution containing H_2ase under aerobic conditions; $Ru(bpy)_3^{2+}$ and MV^{2+} were then immobilized to provide the ternary component system RMH-PGP50. The amounts of the immobilized components were estimated from the absorption spectra of the soaking solutions (Figure S4 in the Supporting Information).

Figure 1d−e shows typical photographs of MV^{2+} photoreduction in the binary system, RM-PGP50, with EDTA. Upon irradiation with solar-simulated light (100 mW cm^{-2}, Figure S1 in the Supporting Information) under aerobic conditions, the color of RM-PGP50 (Figure 1d), immersed in a solution containing EDTA (20 mM) acting as a sacrificial electron donor, changed from yellowish to black, even inside of the PGP50 (Figure 1e, Figure S5e in the Supporting Information); this finding confirmed the accumulation of the reduced form, $MV^{\bullet+}$, in RM-PGP50. The absorbance of RM-PGP50 at 600 nm ($MV^{\bullet+}$) significantly increased with the irradiation time (trace a in Figure 2). Having reached a plateau after 30 min, the

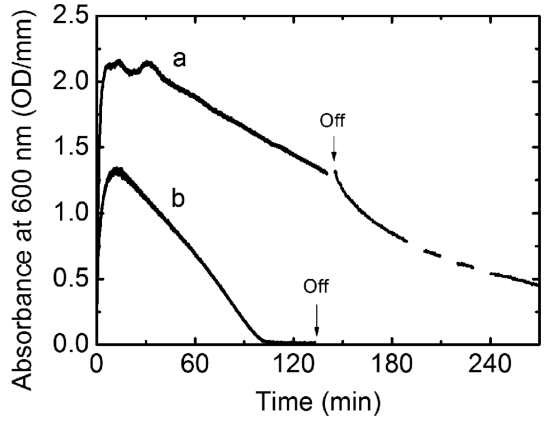

Figure 2. Accumulation of $MV^{\bullet+}$ in a nanoporous glass plate. Changes in absorbance at 600 nm of $MV^{\bullet+}$ upon irradiation were measured under aerobic conditions in RM-PGP50 (thickness: 0.5 mm) immersed in a solution containing EDTA (line a) and in a solution of 0.1 M Tris-HCl (pH7.4) containing 0.5 mM $Ru(bpy)_3^{2+}$, 3 mM MV^{2+} and 20 mM EDTA (line b). The amount of adsorbed $Ru(bpy)_3^{2+}$ and MV^{2+} were 2.9 ± 0.4 and 22 ± 5 μmol/g PGP50, respectively. The word "off" indicates the time at which the irradiation was turned off. Photoreactions were performed in a 1 mm quartz cuvette without sealing and stirring.

absorbance gradually decreased. This was possibly due to oxidation by molecular oxygen penetrating into the nanopores from the solution and by the decrease in EDTA concentration in the quartz reaction cuvette (1 mm path length). Possibilities of desorption of $MV^{2+/\bullet+}$ from the RM-PGP50 and influence of reactive oxygen species might be involved in the decrease in the absorbance. The amount of $MV^{\bullet+}$ decreased gradually after the cessation of irradiation. In cross sections, the dark color of $MV^{\bullet+}$ diminished from both sides of the plate, while the central region retained the dark color for a few hours (Figure S5f in the Supporting Information). $MV^{\bullet+}$ in the RM-PGP50 was stable against vigorous stirring (Figure S6 in the Supporting Information). These observations suggest that the nanopores can resist the influx of O_2 into the interior of RM-PGP50, where a reductive environment was established by the accumulation of $MV^{\bullet+}$ that reduces O_2 penetrating from the outer medium. As shown in Figure 2, trace b, a control experiment was performed, in which a solution containing $Ru(bpy)_3^{2+}$, MV^{2+}, and EDTA but without PGP, was irradiated. $MV^{\bullet+}$ was initially formed but was then completely oxidized by molecular oxygen diffusing by convection flow inside the solution. These results indicate that under aerobic external conditions, $MV^{\bullet+}$ accumulated in the nanoporous interior of PGP50 for a long time because of the slow influx of O_2 from the outer medium. Achieved reductive environments in nanopores may also result in the stabilization of the excited state of $Ru(bpy)_3^{2+*}$.[28]

dx.doi.org/10.1021/jz5008164 | J. Phys. Chem. Lett. 2014, 5, 2402−2407

Negligible H_2 production was observed for the previously mentioned RM-PGP50 and solution systems under aerobic conditions. Production of H_2 from the solution system containing $Ru(bpy)_3^{2+}$, MV^{2+}, H_2ase, and EDTA upon light irradiation was also negligible under aerobic conditions (Figure 3 (■) and Table 1, entry 6). In contrast, the ternary system,

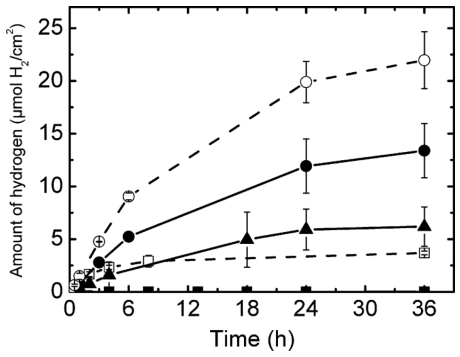

Figure 3. Time evolution of light-driven hydrogen production by RMH-PGP50 (●, 0.5 mm thick; ▲, 1.0 mm thick) and a solution (■) containing 0.1 M Tris-HCl (pH 7.4), 0.5 mM $Ru(bpy)_3^{2+}$, 3 mM MV^{2+}, 5.5 μM H_2ase, and 20 mM EDTA under aerobic conditions. Empty symbols (○ and □) represent experiments performed under anaerobic conditions for RMH-PGP50 (thickness: 0.5 mm) and the solution system, respectively. The amounts of $Ru(bpy)_3^{2+}$, MV^{2+}, and H_2ase inside PGP50s are described in Table 1.

RMH-PGP50 (thickness: 0.5 mm) with EDTA, showed significant production of H_2 (Figure 3 (●) and Table 1, entry 3), that is, 3300-fold higher than that in the solution system after 36 h of irradiation. No H_2 production was observed for a solution system, where the concentration of the catalytic components was adjusted to those in nanopores of RMH-PGP50 (Table S1 in the Supporting Information, entries 1 and 9). Under anaerobic conditions, the amount of H_2 production increased for both the solution (□) and the RMH-PGP50 systems (○), indicating that the presence of O_2 can cause a reduction of H_2 production and that the nanoporous environment can facilitate the photoinduced catalytic reaction.

Table 1 lists the amount of immobilized H_2ase in PGP50, the H_2 evolution activity. Comprehensive data including the conversion efficiency estimated from the photon flux density are summarized in Table S1 in the Supporting Information. In nanoporous PGP50 (thickness: 0.5 mm), the ternary redox components are densely immobilized (9.1 ± 1.2 and 68 ± 14 mM in the nanopores for $Ru(bpy)_3^{2+}$ and MV^{2+}, respectively) to achieve an efficient photoinduced electron transfer. The slightly lower activity that we determined under aerobic external conditions (7.9 ± 0.3 mol H_2 (mol H_2ase)$^{-1}$ s^{-1}, entry 1 to compare with 11 ± 1 mol H_2 (mol H_2ase)$^{-1}$ s^{-1} under anaerobic external conditions) confirms that PGP50 provides reductive interiors. The hydrogen evolution activity is 370 times higher than that reported for Ru-linked [NiFe]-H_2ase (from *Thiocapsa roseopersicina*, 98 kDa[29]) in the presence of oxygen (13.5 nmol H_2 (mg H_2ase)$^{-1}$ min^{-1}, equal to 0.0221 mol H_2 (mol H_2ase)$^{-1}$ s^{-1})[6] and comparable to that of Ru/TiO_2-modified [NiFeSe]-H_2ase (from *Desulfomicrobium baculatum*, ~10 mol H_2 (mol H_2ase)$^{-1}$ s^{-1}), which was obtained after being exposed to air for 72 h,[5] although such comparison with different types of H_2ases is not simple. The turnover number (TON) of H_2ase in RMH-PGP50 was evaluated to be (1.3 ± 0.6) × 10^5 after irradiation for 12 h under aerobic conditions (entry 1). Remarkably, even under aerobic external conditions, the H_2 evolution rate per unit area of RMH-PGP50 was significantly larger than that reported for PSI-H_2ase conjugate measured under anaerobic conditions (entry 2), 3.7 μmol H_2 m^{-2} s^{-1}, 0.36% of conversion efficiency (Table S1 in the Supporting Information, entry 2) compared with 1.2 μmol H_2 m^{-2} s^{-1}.[8]

When a thicker PGP50 (thickness: 1.0 mm) was used under aerobic external conditions, the activity decreased (Figure 3 (▲) and entry 4) as compared with that of a thinner PGP50 (0.5 mm in thickness (●) and entry 3). While the photoreduction rate of MV^{2+} in 0.5-mm-PGP50 was comparable to that in 1-mm-PGP50 (~20 μmol m^{-2} s^{-1}), conversion efficiency from $MV^{\bullet+}$ to H_2 for 0.5-mm-PGP50 was measured to be 2.9 times higher than that of 1-mm-PGP50. It was also found that the distribution of H_2ase inside PGP50s was heterogeneous, unlike that of $Ru(bpy)_3^{2+}$ and MV^{2+} (Figure S7 in the Supporting Information). In the 0.5-mm- and 1-mm-PGP50s (b and c), the central region contained a smaller amount of rhodamine-labeled H_2ase (Rh-H_2ase). The analysis of these distribution profiles together with that of photographic images of cross-sections of PGP50s (Figure S7 in the Supporting Information) suggests that the concentration of Rh-H_2ase in the central region of 0.5 mm-PGP50 is higher than that in 1-mm-PGP50. It is likely that H_2ase, if located further away from the plate surfaces, can react with $MV^{\bullet+}$ more efficiently, thereby producing H_2 even under aerobic external

Table 1. Amount of Adsorbed Hydrogenase (H_2ase) in PGP50 and H_2 Production Activities

				H_2 evolution activity (mol H_2 (mol H_2ase)$^{-1}$ s^{-1})		rate of H_2 evolution/area (μmol H_2 m^{-2} s^{-1})	
entry	photoreaction system	thickness of PGP (mm)	adsorbed H_2ase (nmol g^{-1} PGP50)	anaerobic	aerobic	anaerobic	aerobic
1	RMH-PGP50	0.5[a]	0.27	11 ± 1	7.9 ± 0.3	2.0 ± 0.3	1.3 ± 0.1
2			12.9 ± 0.2	0.85 ± 0.17	0.48 ± 0.03	5.6 ± 1.1	3.7 ± 0.2
3			55 ± 5	0.14 ± 0.03	(8.1 ± 0.2) × 10^{-2}	4.7 ± 0.8	2.7 ± 0.1
4		1.0[b]	27 ± 6	0.22 ± 0.07	(3.1 ± 0.7) × 10^{-2}	6.9 ± 1.9	0.97 ± 0.25
5		1.0[b,c]	3.3 × 10^{-2}	24 ± 6	3.5 ± 0.9	1.3 ± 0.2	0.15 ± 0.03
6	RMH solution[d]			0.72 ± 0.12	n.d.[e]	2.9 ± 0.9	(1.4 ± 0.7) × 10^{-3}

[a]Amount of adsorbed $Ru(bpy)_3^{2+}$ and MV^{2+} was 2.9 ± 0.4 and 22 ± 5 μmol g^{-1} PGP50, respectively. The concentrations of $Ru(bpy)_3^{2+}$ and MV^{2+} in nanopores of PGP50 were estimated to be 9.1 ± 1.2 and 68 ± 14 mM, respectively. [b]Amount of adsorbed $Ru(bpy)_3^{2+}$ and MV^{2+} was 3.0 ± 0.1 and 17 ± 1 μmol g^{-1} PGP50, respectively. The concentration of $Ru(bpy)_3^{2+}$ and MV^{2+} in nanopores of PGP50 was estimated to be 9.4 ± 0.2 and 54 ± 3 mM, respectively. [c]Solution of MES-NaOH (0.1 M, pH 6.6) containing 20 mM EDTA was used for soaking and H_2 production assay. [d]Concentration of $Ru(bpy)_3^{2+}$, MV^{2+}, and H_2ase was 0.5 mM, 3 mM, and 5.5 μM, respectively. [e]Not determined.

dx.doi.org/10.1021/jz5008164 | J. Phys. Chem. Lett. 2014, 5, 2402−2407

condition. This is probably due to penetration of oxygen in regions near the surface. Although a thinner PGP50 (thickness: 0.2 mm) homogeneously adsorbed a larger amount of H_2ase (96 ± 21 nmol g^{-1}, Figure S7a in the Supporting Information), it could not adsorb $Ru(bpy)_3^{2+}$ or MV^{2+}, resulting in a negligible H_2 production (data not shown).

Under anaerobic conditions, H_2ase absorbed in the near-surface region can significantly contribute to the production of hydrogen. In particular, the optimized RMH-PGP50 showed significant H_2 production efficiency at 24 mol H_2 (mol H_2ase)$^{-1}$ s^{-1} (entry 5 and refer to the activity via reaction with MV^{2+}/dithionite described in Supporting Information). The TON of H_2ase in RMH-PGP50 was evaluated to be 2.2 × 10^5 during irradiation for 4 h, suggesting that the nanopore hosts H_2ase to maintain its activity for a longer time. The maximum conversion efficiency was measured to be 1.3% at the highest amount of adsorbed H_2ase in this study (Table S1 in the Supporting Information, entry 8). The conversion efficiency from $MV^{\bullet+}$ to H_2 and the quantum yield estimated from photon numbers absorbed by $Ru(bpy)_3^{2+}$ were estimated to be 78 and 3.7%, respectively. The latter value is comparable to that achieved by semiconductor systems, 6.3%.[30] Activity of H_2 production by MV^{2+}/H_2ase immobilized in PGP50 with dithionite is much higher than that of the photocatalytic RMH-PGP50 system, suggesting that the possibility of product inhibition can be excluded. Taken together, the electron-transfer process from $Ru(bpy)_3^{2+}$ to MV^{2+} determines the efficiency of the light-driven H_2 production under the H_2ase-rich condition.

PGPs with pore diameter equal to 20 or 75 nm were found to be less effective for the production of H_2 (<8% of PGP50). Unfortunately, a clear explanation for this result could not be found. The efficiency of H_2 production of RMH-PGP50 strongly depended on the pH (6.2 to 7.8) of the outer medium; for example, a reduction from pH 7.4 to 6.6 increased the efficiency of H_2 production of ∼80% (data not shown). In contrast, the activity was found to be independent of the ionic strength (at 0−100 mM NaCl). Thus, the main factors that determine the efficiency of H_2 production are likely due to the stabilization of H_2ase, the electron transfer rate from $Ru(bpy)_3^{2+}$ to MV^{2+}, and the pH inside the nanopore.

Notably, H_2ase in RMH-PGP50 is robust enough to be reused under aerobic conditions. H_2 evolution was observed without any significant deactivation of the enzyme (Figure S8 in the Supporting Information) during a 36 h catalytic photoreaction until EDTA was fully consumed. This result indicates that H_2ase is highly stable inside PGP50. As shown in previous studies with photosynthetic pigment−protein complexes conjugated inside porous silicate materials,[20−22] EDTA can be supplied from the outer medium, although its penetration rate into nanopores should be carefully taken into account in each case. The RMH-PGP50 system therefore offers the possibility of building a new bio-H_2 reactor that allows continuous supply of EDTA or other reagents using a flow system without degassing.

One of the most important findings of this study is that we have shown how an anaerobic environment can be automatically established by a local photoreduction of MV^{2+} inside nanopores even under aerobic exterior environments. In the nanopore environment, the fragile H_2ase can ensure a long-term activity (TON = (1.3 ± 0.6) × 10^5 for 12 h). The proposed catalytic PGP system is easy to prepare and offers a basis for the construction of new platforms for the O_2-sensitive, light-driven, chemical conversion systems that allow easily regulated exchanges of reactants and products between the outer medium and active components immobilized inside the nanopores. Our methodology can be also employed to immobilize photocatalytic proteins, such as the reaction center complexes of photosynthetic photosystems I and II (PSI and PSII), which have been shown to be fully active inside silica nanopores in mesoscopic materials.[20,21] This type of mild immobilization will be useful because it affects the local molecular motion mildly and the long-range molecular motion/diffusion depending on the molecular size of the reactants and products. Combination of H_2ase, PGP, and these photoactive electron-donating pigment−proteins will be useful for the light-driven hydrogen production devices employing water-splitting reaction systems.

■ EXPERIMENTAL METHODS

Preparation of $Ru(bpy)_3^{2+}$/MV^{2+}/Hydrogenase-Immobilized PGP50 (RMH-PGP50). All preparations were performed under aerobic conditions. A PGP50 substrate (thickness: 0.2, 0.5, or 1.0 mm) was immersed in a hydrogenase-containing medium (0.005, 0.02, 1.4, 5.5, or 55 μM hydrogenase; 25 mM Tris-HCl (pH 7.4); or 25 mM MES-NaOH (pH 6.6)) at 4 °C for 24 h. The amount of hydrogenase adsorbed onto PGP50 was determined from the decrease in absorbance of the soaking solution at 400 nm using a spectrophotometer (UV-1800; Shimadzu) (Figure S4 in the Supporting Information). The resulting hydrogenase-PGP50 (H-PGP50) was then immersed into the medium (0.1 M Tris-HCl, pH 7.4 or 0.1 M MES-NaOH, pH 6.6) containing 0.5 mM $Ru(bpy)_3^{2+}$, 3 mM MV^{2+}, and 20 mM EDTA·2Na at 4 °C for 24 h. The amount of $Ru(bpy)_3^{2+}$ and MV^{2+} adsorbed onto the PGP were determined from the decrease in absorbance of $Ru(bpy)_3^{2+}$ and MV^{2+} in the soaking solution by spectrophotometry (Figure S4 in the Supporting Information). The resulting $Ru(bpy)_3^{2+}$(R)/MV^{2+}(M)/hydrogenase(H)-immobilized PGP50 (RMH-PGP50) was rinsed with a solution of 100 mM Tris-HCl (pH 7.4) containing 20 mM EDTA·2Na or 100 mM MES-NaOH (pH 6.6) containing 20 mM EDTA·2Na.

Photoreduction Assay of MV^{2+}. Photoreduction of MV^{2+} in $Ru(bpy)_3^{2+}$(R)/MV^{2+}(M)-immobilized PGP50 (RM-PGP50: 0.5 mm thickness) was measured under aerobic conditions using a spectrometer (EPP2000-UVN-SR; StellarNet). RM-PGP50 was immersed in a solution of Tris-HCl (0.1 M, pH 7.4) containing 20 mM EDTA·2Na and then irradiated with a solar simulator (100 mW cm^{-2}) (OTENTO-SUN II; Bunkoukeiki). The absorbance at 600 nm was monitored using the irradiation light as a probe light source. As a control experiment, a solution of $Ru(bpy)_3^{2+}$ (0.5 mM) and MV^{2+} (3 mM) in a reaction vessel was measured using a method similar to that employed for RM-PGP50. The absorbance under dark conditions was measured using a deuterium/halogen lamp (SL5; StellarNet) as the probe light source, using a fiber-optic cable (F600-UVVis-SR; StellarNet). Density of photon flux generated by the solar simulator was measured in the range of 400−700 nm using a spectrometer (EPP2000-UVN-SR; StellarNet). The spectrometer sensitivity was corrected by a standard light source (SL1-CAL, StellarNet).

Light-Driven H_2 Production Assay. Unless otherwise stated, all procedures were performed under aerobic conditions. The total volume of the reaction cell was 6.7 or 7.6 mL. The volume of the reaction medium of RMH-PGP50 (thickness: 0.2, 0.5, or 1.0 mm) was adjusted to 3, 7.5, and 15 mg/mL. RMH-PGP50

dx.doi.org/10.1021/jz5008164 | J. Phys. Chem. Lett. 2014, 5, 2402−2407

was irradiated using a solar simulator (100 mW cm^{-2}) (OTENTO-SUN II; Bunkoukeiki). From the headspace of the reaction cell, 500 μL of gas were collected using a gastight syringe, followed by GC analysis. Shimadzu GC-14B was equipped with a packed column of 60/80 mesh-activated charcoal using a thermal conductivity detector. The H_2 concentration was calibrated in advance. Experiments under anaerobic conditions were carried out by N_2 bubbling (1 h) of a solution in which RMH-PGP50 was immersed; the cuvette was purged with N_2. Rate of H_2 evolution/area (μmol H_2 m^{-2} s^{-1}) was calculated from the light-receiving areas of 2.5 cm^2 for the solution system (0.2 mL solution) and 20.1 (or 16.8) and 9.27 (or 8.4) cm^2 g^{-1} for the 0.5-mm- and 1.0-mm-PGP50 systems, respectively. In the absence of H_2ase, H_2 production was negligible under aerobic conditions; however, detectable H_2 production was observed for RM-PGP50 under anaerobic conditions; 0.16, 0.42, and 0.45 μmol H_2 m^{-2} s^{-2} for 0.5-mm-RM-PGP50 (pH7.4) and 1.0-mm-RM-PGP50 (pH 7.4 and 6.6), respectively. Thus, the rate of H_2 evolution/area (μmol H_2 m^{-2} s^{-1}) by RMH-PGP50 was corrected by subtraction of the contribution from RM-PGP50s as baselines, then H_2 evolution activity (mol H_2 (mol H_2ase)$^{-1}$) was evaluated. The conversion efficiency was evaluated as 2 × [rate of H_2 evolution per area (μmol m^{-2} s^{-1})]/[rate of reduction of MV^{2+} per area (μmol m^{-2} s^{-1})]. The quantum yield was evaluated as 2 × [rate of H_2 evolution per area (μmol m^{-2} s^{-1})]/[number of absorbed photons by $Ru(bpy)_3^{2+}$ per area (μmol m^{-2} s^{-1})].

■ ASSOCIATED CONTENT

Supporting Information

Experimental methods, table of hydrogen production activity, and figures displaying the characterization of RMH-PGP50s and time evolution of H_2 production by RMH-PGP50 with/without irradiation. This material is available free of charge via the Internet at http://pubs.acs.org.

■ AUTHOR INFORMATION

Corresponding Authors

*E-mail: tnoji@nitech.ac.jp (T.N.).
*E-mail: takedewa@nitech.ac.jp (T.D.).

Notes

The authors declare no competing financial interest.

■ ACKNOWLEDGMENTS

This work was partially supported by PRESTO (Japan Science and Technology Agency, JST). T.D. and T.N. thank Tatematsu, Takahashi, and Hibi Foundation for funding. M.N. and T.D. thank AOARD for funding. We are grateful to Professor Yutaka Amao for helpful comments and discussion. T.N. and T.D. thank Professors Takeo Matsumoto and Kazuaki Nagayama and Mr. Junfeng Wang for the measurements of Rh-H_2ase immobilized in PGP50 carried out with confocal scanning laser scanning microscope. S.I. thanks Professor Masahiro Ishiura for valuable discussion. We thank Mr. Kojiro Endo for his excellent assistance with the experiments in the early stages of this project.

■ REFERENCES

(1) Friedrich, B. R.; Fritsch, J.; Lenz, O. Oxygen-Tolerant Hydrogenases in Hydrogen-Based Technologies. *Curr. Opin. Biotechnol.* **2011**, *22*, 358−364.

(2) Esper, B.; Badura, A.; Rogner, M. Photosynthesis as a Power Supply for (Bio-)hydrogen Production. *Trends Plant Sci.* **2006**, *11*, 543−549.

(3) De Lacey, A. L.; Fernandez, V. M.; Rousset, M.; Cammack, R. Activation and Inactivation of Hydrogenase Function and the Catalytic Cycle: Spectroelectrochemical Studies. *Chem. Rev.* **2007**, *107*, 4304−4330.

(4) Hambourger, M.; Gervaldo, M.; Svedruzic, D.; King, P. W.; Gust, D.; Ghirardi, M.; Moore, A. L.; Moore, T. A. [FeFe]-Hydrogenase-Catalyzed H_2 Production in a Photoelectrochemical Biofuel Cell. *J. Am. Chem. Soc.* **2008**, *130*, 2015−2022.

(5) Reisner, E.; Powell, D. J.; Cavazza, C.; Fontecilla-Camps, J. C.; Armstrong, F. A. Visible Light-Driven H_2 Production by Hydrogenases Attached to Dye-Sensitized TiO_2 Nanoparticles. *J. Am. Chem. Soc.* **2009**, *131*, 18457−18466.

(6) Zadvornyy, O. A.; Lucon, J. E.; Gerlach, R.; Zorin, N. A.; Douglas, T.; Elgren, T. E.; Peters, J. W. Photo-Induced H_2 Production by [NiFe]-Hydrogenase from *T. roseopersicina* Covalently Linked to a Ru(II) photosensitizer. *J. Inorg. Biochem.* **2012**, *106*, 151−155.

(7) Lubner, C. E.; Applegate, A. M.; Knorzer, P.; Ganago, A.; Bryant, D. A.; Happe, T.; Golbeck, J. H. Solar Hydrogen-Producing Bionanodevice Outperforms Natural Photosynthesis. *Proc. Natl. Acad. Sci. U. S. A.* **2011**, *108*, 20988−20991.

(8) Krassen, H.; Schwarze, A.; Friedrich, B.; Ataka, K.; Lenz, O.; Heberle, J. Photosynthetic Hydrogen Production by a Hybrid Complex of Photosystem I and [NiFe]-hydrogenase. *ACS Nano* **2009**, *3*, 4055−4061.

(9) Iwuchukwu, I. J.; Vaughn, M.; Myers, N.; O'Neill, H.; Frymier, P.; Bruce, B. D. Self-Organized Photosynthetic Nanoparticle for Cell-Free Hydrogen Production. *Nat. Nanotechnol.* **2010**, *5*, 73−79.

(10) Silver, S. C.; Niklas, J.; Du, P.; Poluektov, O. G.; Tiede, D. M.; Utschig, L. M. Protein Delivery of a Ni Catalyst to Photosystem I for Light-Driven Hydrogen Production. *J. Am. Chem. Soc.* **2013**, *135*, 13246−13249.

(11) Utschig, L. M.; Silver, S. C.; Mulfort, K. L.; Tiede, D. M. Nature-Driven Photochemistry for Catalytic Solar Hydrogen Production: a Photosystem I-Transition Metal Catalyst Hybrid. *J. Am. Chem. Soc.* **2011**, *133*, 16334−16337.

(12) Utschig, L. M.; Dimitrijevic, N. M.; Poluektov, O. G.; Chemerisov, S. D.; Mulfort, K. L.; Tiede, D. M. Photocatalytic Hydrogen Production from Noncovalent Biohybrid Photosystem I/Pt Nanoparticle Complexes. *J. Phys. Chem. Lett.* **2011**, *2*, 236−241.

(13) Berggren, G.; Adamska, A.; Lambertz, C.; Simmons, T. R.; Esselborn, J.; Atta, M.; Gambarelli, S.; Mouesca, J. M.; Reijerse, E.; Lubitz, W.; et al. Biomimetic Assembly and Activation of [FeFe]-Hydrogenases. *Nature* **2013**, *499*, 66−69.

(14) Goldet, G.; Wait, A. F.; Cracknell, J. A.; Vincent, K. A.; Ludwig, M.; Lenz, O.; Friedrich, B.; Armstrong, F. A. Hydrogen Production under Aerobic Conditions by Membrane-Bound Hydrogenases from Ralstonia Species. *J. Am. Chem. Soc.* **2008**, *130*, 11106−11113.

(15) Shafaat, H. S.; Rudiger, O.; Ogata, H.; Lubitz, W. [NiFe] Hydrogenases: A Common Active Site for Hydrogen Metabolism under Diverse Conditions. *Biochim. Biophys. Acta* **2013**, *1827*, 986−1002.

(16) Pandelia, M.-E.; Fourmond, V.; Tron-Infossi, P.; Lojou, E.; Bertrand, P.; Léger, C.; Giudici-Orticoni, M.-T.; Lubitz, W. Membrane-Bound Hydrogenase I from the Hyperthermophilic Bacterium Aquifex aeolicus: Enzyme Activation, Redox Intermediates and Oxygen Tolerance. *J. Am. Chem. Soc.* **2010**, *132*, 6991−7004.

(17) Ciaccafava, A.; De Poulpiquet, A.; Techer, V.; Giudici-Orticoni, M. T.; Tingry, S.; Innocent, C.; Lojou, E. an Innovative Powerful and Mediatorless H_2/O_2 Biofuel Cell Based on an Outstanding Bioanode. *Electrochem. Commun.* **2010**, *23*, 25−28.

(18) De Poulpiquet, A.; Ciaccafava, A.; Szot, K.; Pillain, B.; Infossi, P.; Guiral, M.; Opallo, M.; Giudici-Orticoni, M.-T.; Lojou, E. Exploring Properties of a Hyperthermophilic Membrane-Bound Hydrogenase at Carbon Nanotube Modified Electrodes for a Powerful H_2/O_2Biofuel Cell. *Electroanalysis* **2013**, *25*, 685−695.

(19) Yiu, H. H. P.; Wright, P. A. Enzymes Supported on Ordered Mesoporous Solids: a Special Case of an Inorganic-Organic Hybrid. *J. Mater. Chem.* **2005**, *15*, 3690−3700.
(20) Kamidaki, C.; Kondo, T.; Noji, T.; Itoh, T.; Yamaguchi, A.; Itoh, S. Alumina Plate Containing Photosystem I Reaction Center Complex Oriented inside Plate-Penetrating Silica Nanopores. *J. Phys. Chem. B* **2013**, *117*, 9785−9792.
(21) Noji, T.; Kamidaki, C.; Kawakami, K.; Shen, J. R.; Kajino, T.; Fukushima, Y.; Sekitoh, T.; Itoh, S. Photosynthetic Oxygen Evolution in Mesoporous Silica Material: Adsorption of Photosystem II Reaction Center Complex into 23 nm Nanopores in SBA. *Langmuir* **2011**, *27*, 705−713.
(22) Oda, I.; Iwaki, M.; Fujita, D.; Tsutsui, Y.; Ishizaka, S.; Dewa, M.; Nango, M.; Kajino, T.; Fukushima, Y.; Itoh, S. Photosynthetic Electron Transfer from Reaction Center Pigment-Protein Complex in Silica Nanopores. *Langmuir* **2010**, *26*, 13399−13406.
(23) Yazawa, T.; Tanaka, H.; Eguchi, K.; Yokoyama, S. Novel Alkali-Resistant Porous-Glass Prepared from a Mother Glass Based on the SiO_2-B_2O_3-RO-ZrO_2 (R=Mg, Ca, Sr, Ba and Zn). *J. Mater. Sci.* **1994**, *29*, 3433−3440.
(24) Tanaka, H.; Yazawa, T.; Eguchi, K.; Nagasawa, H.; Matsuda, N.; Einishi, T. Precipitation of Colloidal Silica and Pore-Size Distribution in High Silica Porous-Glass. *J. Non-Cryst. Solids* **1984**, *65*, 301−309.
(25) Yazawa, T. Nanopore Glass. In *Nanoporous Materials: Synthesis and Its Applications*; Xiu, Q., Ed.; CRC Press (Taylor & Francis Group): New York, 2013; pp 289−318.
(26) Higuchi, Y.; Yasuoka, N.; Kakudo, M.; Katsube, Y.; Yagi, T.; Inokuchi, H. Single Crystals of Hydrogenase from *Desulfovibrio vulgaris* Miyazaki F. *J. Biol. Chem.* **1987**, *262*, 2823−2825.
(27) Okura, I.; Kim-Thuan, N. Hydrogen Generation by Visible Light with Tris-(2,2′-bipyridine) Ruthenium Dication. *J. Mol. Catal.* **1979**, *5*, 311−314.
(28) Wolfgang, S.; Gafney, H. D. Quenching of Tris(2,2′-bipyridine)ruthenium(II) ($Ru(bpy)_3^{2+}$) Ionically Bound to Porous Vycor Glass by Oxygen, Nitrous Oxide, and Sulfur Dioxide. *J. Phys. Chem.* **1983**, *87*, 5395−5401.
(29) Kovacs, K. L.; Tigyi, G.; Thanh, L. T.; Lakatos, S.; Kiss, Z.; Bagyinka, C. Structural Rearrangements in Active and Inactive forms of Hydrogenase from *Thiocapsa roseopersicina*. *J. Biol. Chem.* **1991**, *266*, 947−951.
(30) Maeda, K.; Domen, K. Photocatalytic Water Splitting: Recent Progress and Future Challenges. *J. Phys. Chem. Lett.* **2010**, *1*, 2655−2611.